J. Plasma Phys. (2020), *vol.* 86, 825860302
Published by Cambridge University Press
doi:10.1017/S0022377820000604

A family of Vlasov–Maxwell equilibrium distribution functions describing a transition from the Harris sheet to the force-free Harris sheet

T. Neukirch[1,†], **F. Wilson**[1] **and O. Allanson**[2]

[1]School of Mathematics and Statistics, University of St Andrews, St Andrews KY16 9SS, UK

[2]Space and Atmospheric Electricity Group, Department of Meteorology, University of Reading, Reading RG6 6BB, UK

(Received 30 March 2020; revised 20 May 2020; accepted 21 May 2020)

We discuss a family of Vlasov–Maxwell equilibrium distribution functions for current sheet equilibria that are intermediate cases between the Harris sheet and the force-free (or modified) Harris sheet. These equilibrium distribution functions have potential applications to space and astrophysical plasmas. The existence of these distribution functions had been briefly discussed by Harrison & Neukirch (*Phys. Rev. Lett.*, vol. 102, (2009*a*), 135003), but here it is shown that their approach runs into problems in the limit where the guide field goes to zero. The nature of this problem will be discussed and an alternative approach will be suggested that avoids the problem. This is achieved by considering a slight variation of the magnetic field profile, which allows a smooth transition between the Harris and force-free Harris sheet cases.

Key words: astrophysical plasmas, space plasma physics

1. Introduction

Current sheets are important for the structure and dynamical behaviour of many plasma systems. In space and astrophysical plasmas current sheets play a crucial role in magnetic activity processes by, for example, aiding the release of magnetic energy by magnetic reconnection. Current sheet equilibria are often used as starting points for studying the dynamic behaviour of plasmas in, e.g. the solar atmosphere, the solar wind and planetary magnetospheres.

Many astrophysical plasmas can be described as collisionless and in this case the relevant equilibria are solutions of the steady-state Vlasov–Maxwell (VM) equations (e.g. Schindler 2007). Since current sheets are strongly localised in space, they can often be well approximated by one-dimensional (1-D) models (see, e.g. Roth, de Keyser & Kuznetsova 1996; Zelenyi *et al.* 2011; Kocharovsky *et al.* 2016; Neukirch, Wilson & Allanson 2018). An often used example of a 1-D current sheet model is the Harris sheet (Harris 1962), which is a neutral sheet model that

† Email address for correspondence: tn3@st-andrews.ac.uk

has been used extensively in studies of, e.g. magnetic reconnection (e.g. Kuznetsova, Hesse & Winske 1998; Shay *et al.* 1998; Hesse *et al.* 1999; Kuznetsova, Hesse & Winske 2000, 2001; Hesse, Birn & Kuznetsova 2001; Pritchett 2001; Rogers, Denton & Drake 2003; Hesse, Kuznetsova & Birn 2004; Pritchett & Coroniti 2004; Ricci *et al.* 2004; Hesse *et al.* 2005; Pritchett 2005; Hesse 2006; Daughton & Karimabadi 2007; Wan *et al.* 2008; Daughton *et al.* 2011; Hesse *et al.* 2011).

In some plasma systems, it can be more appropriate to use a current sheet model for which the pressure gradient is negligible. Such models are termed force free, and satisfy the condition $\boldsymbol{j} \times \boldsymbol{B} = 0$, i.e. the current density $\boldsymbol{j}$ and magnetic field $\boldsymbol{B}$ are aligned with each other.

The Harris sheet magnetic field is kept in force balance by a pressure gradient, but one can also keep the system in a macroscopic force balance by adding a non-uniform guide field to the system while the plasma pressure is constant. The resulting configuration is often called the force-free Harris sheet. Equilibrium distribution functions (DFs) for this configuration have been found, for example, by Harrison & Neukirch (2009*a*), Neukirch, Wilson & Harrison (2009), Wilson & Neukirch (2011), Abraham-Shrauner (2013), Kolotkov, Vasko & Nakariakov (2015), Dorville *et al.* (2015), Allanson *et al.* (2015, 2016), Wilson, Neukirch & Allanson (2017, 2018) and Neukirch *et al.* (2020) (for further references on force-free Vlasov–Maxwell equilibria, see e.g. Moratz & Richter 1966; Sestero 1967; Channell 1976; Correa-Restrepo & Pfirsch 1993; Attico & Pegoraro 1999; Bobrova *et al.* 2001; Harrison & Neukirch 2009*b*; Vasko *et al.* 2014).

Similarly to the Harris sheet, collisionless force-free configurations have been used as initial conditions for particle-in-cell simulations of collisionless reconnection, using for example the exact equilibrium by Harrison & Neukirch (2009*a*) (e.g. Wilson *et al.* 2016), linear force-free equilibria (e.g. Bobrova *et al.* 2001; Nishimura *et al.* 2003; Bowers & Li 2007) or approximate force-free equilibria (e.g. Hesse *et al.* 2005; Liu *et al.* 2013; Guo *et al.* 2014, 2015; Zhou *et al.* 2015; Fan *et al.* 2016; Guo *et al.* 2016*a*,*b*).

In their paper, Harrison & Neukirch (2009*a*) also discussed the case of collisionless current sheets that are intermediate cases between the Harris sheet and the force-free Harris sheet, i.e. cases for which the macroscopic force balance is provided by a combination of the plasma pressure gradient and the gradient of the magnetic pressure component provided by the non-uniform guide field. These equilibria and their DFs self-consistently describe the transition from the Harris sheet to the force-free Harris sheet (or *vice versa*), but have so far not been studied in any detail. Hence, in this paper we present an investigation of these collisionless current sheet equilibria. As this investigation will show, there are actually some problems with the DFs presented in Harrison & Neukirch (2009*a*), which limit their usefulness in practice. To circumvent these issues, we present a family of slightly modified magnetic field profiles and corresponding DFs which avoid these problems, but still describe a transition between the Harris sheet and force-free Harris sheet as limiting cases.

We remark that in this paper we focus on a case in which the plasma temperature is uniform across the current sheet (i.e. an isothermal case). Distribution functions for non-isothermal force-free current sheets have been found by, e.g. Kolotkov *et al.* (2015), Wilson *et al.* (2017) and Neukirch *et al.* (2020). In principle the analysis carried out here could be generalised to these non-isothermal cases.

The paper is structured as follows; in § 2, we briefly discuss the macroscopic equilibria of the Harris sheet, the force-free Harris sheet and the intermediate cases. We then discuss the corresponding VM equilibrium distribution functions as given by

https://doi.org/10.1017/S0022377820000604 Published online by Cambridge University Press

Harrison & Neukirch (2009*a*) in § 3 and illustrate the problem associated with the intermediate cases in the limit when the guide field amplitude tends to zero. In § 4, we present a modified magnetic field model, which allows us to avoid these problems with the distribution function. We close with our summary and conclusions in § 5.

2. The macroscopic picture: Harris sheet, force-free Harris sheet and intermediate cases

The macroscopic force balance for 1-D collisionless current sheet equilibria, with spatial variation only in the z-direction, is determined by (e.g. Mynick, Sharp & Kaufman 1979; Neukirch *et al.* 2018)

$$\frac{\mathrm{d}}{\mathrm{d}z}\left[\frac{B_x(z)^2+B_y(z)^2}{2\mu_0}+P_{zz}(z)\right]=0. \tag{2.1}$$

For collisionless equilibria, we are usually dealing with a pressure tensor and P_{zz} is the only component of the pressure tensor which contributes to the force balance equation.

In this paper we focus on the family of equilibria defined by

$$\boldsymbol{B}(z)=B_0\left(\tanh(z/L),\,\frac{B_{y0}}{B_0\cosh(z/L)},\,0\right), \tag{2.2}$$

$$P_{zz}(z)=\frac{B_0^2-B_{y0}^2}{2\mu_0\cosh^2(z/L)}+P_b, \tag{2.3}$$

where L represents the half-thickness of the current sheet, and $P_b\geqslant 0$ is a constant background pressure. For completeness, we mention that the current density is given by

$$\boldsymbol{j}(z)=\frac{B_0}{\mu_0 L}\left(\frac{B_{y0}\sinh(z/L)}{B_0\cosh^2(z/L)},\,\frac{1}{\cosh^2(z/L)},\,0\right). \tag{2.4}$$

The case $B_{y0}=0$ gives the Harris sheet (Harris 1962), which is a widely used 1-D VM equilibrium in, e.g. reconnection studies, Often a constant guide field component is added to the Harris sheet field, which is not included in our magnetic field model here. When $B_{y0}=B_0$, we obtain the force-free Harris sheet, for which both the pressure $P_{zz}=P_b$ and the magnetic pressure $(B_x^2+B_y^2)/2\mu_0=B_0^2/2\mu_0$ are constant. For $0<B_{y0}<B_0$ we get intermediate cases between the Harris sheet and the force-free Harris sheet. Figure 1 shows the magnetic field, pressure, and current density profiles for the Harris sheet, two intermediate cases, and force-free Harris sheet. Note that in the figure we have set the background pressure P_b (measured in units of $B_0^2/(2\mu_0)$) to $B_{y0}^2/B_0^2+0.1$.

At the macroscopic level discussed so far, there is no problem with varying B_{y0}/B_0 and in particular with letting this ratio go to 0. This changes, however, when we consider the microscopic picture.

3. The microscopic picture

3.1. *One-dimensional Vlasov–Maxwell equilibria*

We assume a 1-D Cartesian set-up, in which all quantities depend only on the z-coordinate, and consider magnetic field profiles of the form $\boldsymbol{B}=(B_x,\,B_y,\,0)$, for which $\boldsymbol{B}=\nabla\times\boldsymbol{A}$ (for vector potential $\boldsymbol{A}=(A_x,\,A_y,\,0)$). In this paper we will always impose conditions on the microscopic parameters of the DFs such that the electric

https://doi.org/10.1017/S0022377820000604 Published online by Cambridge University Press

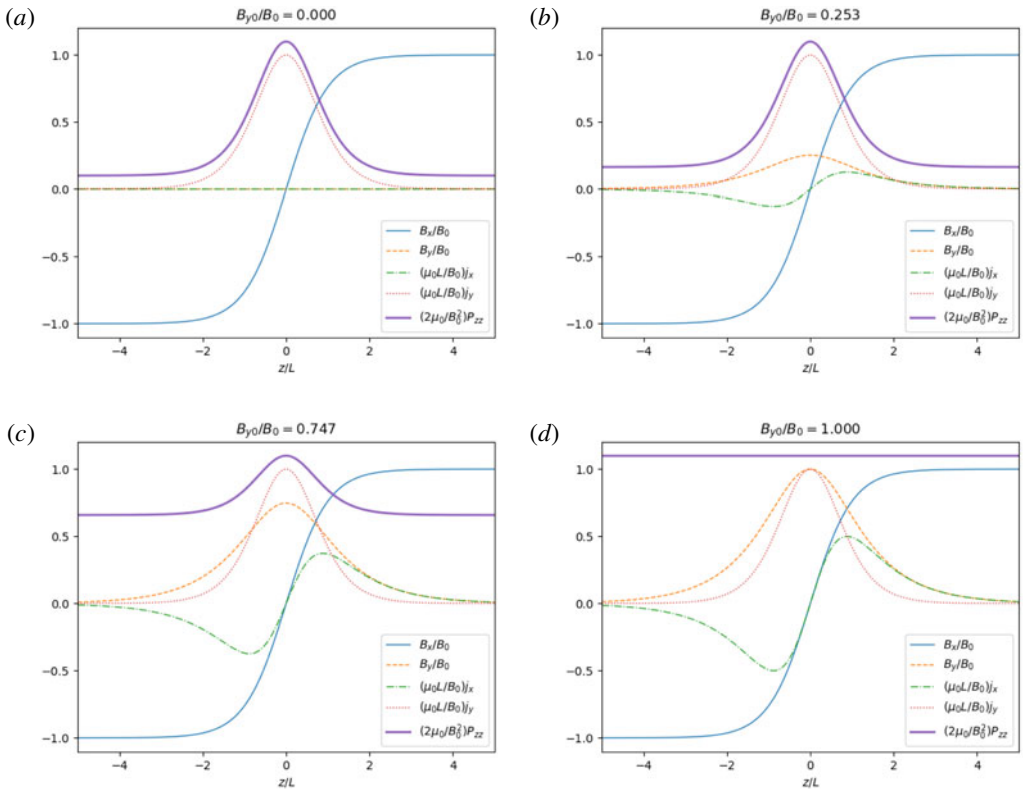

FIGURE 1. Magnetic field, pressure and current density profiles for (*a*) the Harris sheet, (*b*,*c*) intermediate cases with $B_{y0}/B_0 \approx 0.25$ and ≈ 0.75, respectively, and (*d*) the force-free Harris sheet. The background pressure P_b (measured in units of $B_0^2/(2\mu_0)$) has been set to $B_{y0}^2/B_0^2 + 0.1$ in each case.

potential ϕ (and hence the electric field) vanishes (this can always be achieved for the cases we discuss here, see e.g. Neukirch *et al.* 2018). On the microscopic level, we assume that the distributions functions, f_s, are functions of the particle energy, $H_s = m_s(v_x^2 + v_y^2 + v_z^2)/2$, and the x- and y-components of the canonical momentum, $\boldsymbol{p}_s = m_s\boldsymbol{v} + q_s\boldsymbol{A}$ (for m_s the mass and q_s the charge of species s, respectively), since these are known constants of motion for a time-independent system with spatial invariance in the x- and y-directions.

Under the assumptions described above, the VM equations reduce to Ampère's law in the form

$$\frac{\mathrm{d}^2 A_x}{\mathrm{d}z^2} = -\mu_0 \frac{\partial P_{zz}}{\partial A_x}, \tag{3.1}$$

$$\frac{\mathrm{d}^2 A_y}{\mathrm{d}z^2} = -\mu_0 \frac{\partial P_{zz}}{\partial A_y}, \tag{3.2}$$

where P_{zz} is the only component of the pressure tensor that plays a role in the force balance of the 1-D equilibrium, defined by

$$P_{zz}(A_x, A_y) = \sum_s m_s \int v_z^2 f_s(H_s, p_{xs}, p_{ys})\, \mathrm{d}^3 v. \tag{3.3}$$

https://doi.org/10.1017/S0022377820000604 Published online by Cambridge University Press

For a specified magnetic field profile, therefore, one needs to determine $P_{zz}(A_x, A_y)$ such that the vector potential associated with the given magnetic field is a solution of Ampère's law. Regarding (3.3) as an integral equation for f_s and solving it, will give DFs that self-consistently reproduce this macroscopic field profile (e.g. Alpers 1969; Channell 1976; Mottez 2003). For some examples of the application of this approach, see Harrison & Neukirch (2009*a*,*b*), Neukirch *et al.* (2009), Wilson & Neukirch (2011), Abraham-Shrauner (2013), Kolotkov *et al.* (2015), Allanson *et al.* (2015, 2016), Wilson *et al.* (2017) and Wilson *et al.* (2018).

3.2. *The distribution functions*

Harrison & Neukirch (2009*a*) used Channell's method (Channell 1976) to find the following DF for the force-free Harris sheet

$$f_s(H_s, p_{xs}, p_{ys}) = \frac{n_{0s}}{(\sqrt{2\pi}v_{th,s})^3} \mathrm{e}^{-\beta_s H_s}[\mathrm{e}^{\beta_s u_{ys} p_{ys}} + a_s \cos(\beta_s u_{xs} p_{xs}) + b_s], \tag{3.4}$$

where n_{0s} is a typical particle density for species s, $\beta_s = (k_\mathrm{b} T_s)^{-1}$ is the usual inverse temperature parameter and $v_{th,s}^2 = k_\mathrm{b} T_s / m_s = (m_s \beta_s)^{-1}$ is the square of the thermal velocity of species s. As discussed in detail in, for example, Neukirch *et al.* (2009), the additional parameters a_s, b_s, u_{xs} and u_{ys} have to satisfy further constraints to (i) have a positive DF ($b_s > a_s \geqslant 0$), (ii) guarantee that the electric potential vanishes and (iii) ensure that the magnetic vector potential associated with the given macroscopic magnetic field is a solution of Ampère's law.

The DF (3.4) is the sum of the Harris sheet DF (Harris 1962) and an additional part, depending on H_s and $p_{x,s}$

$$f_s(H_s, p_{xs}, p_{ys}) = f_{s,\mathrm{Harris}}(H_s, p_{ys}) + \frac{n_{0s}}{(\sqrt{2\pi}v_{th,s})^3} \mathrm{e}^{-\beta_s H_s}(a_s \cos(\beta_s u_{xs} p_{xs}) + b_s), \tag{3.5}$$

where the Harris sheet DF is given by

$$f_{s,\mathrm{Harris}}(H_s, p_{ys}) = \frac{n_{0s}}{(\sqrt{2\pi}v_{th,s})^3} \mathrm{e}^{-\beta_s (H_s - u_{ys} p_{ys})}. \tag{3.6}$$

Harrison & Neukirch (2009*a*) pointed out that by varying a_s the DF (3.4) can in principle describe all the intermediate cases between the force-free and Harris cases and it looks as if in the limit $a_s \to 0$ one should recover the Harris sheet DF.

However, if one looks more carefully one finds that the parameter a_s has to satisfy the relation (similarly to e.g. Neukirch *et al.* 2009)

$$a_s = \frac{B_{y0}^2}{2B_0^2} \exp\left(\frac{u_{xs}^2}{2v_{th,s}^2}\right) \exp\left(\frac{u_{ys}^2}{2v_{th,s}^2}\right), \tag{3.7}$$

where

$$u_{xs}^2 = \frac{4}{B_{y0}^2 \beta_s^2 q_s^2 L^2}. \tag{3.8}$$

This particular form for a_s results from the consistency relations that the distribution functions have to satisfy for the electric potential calculated from the quasi-neutrality

https://doi.org/10.1017/S0022377820000604 Published online by Cambridge University Press

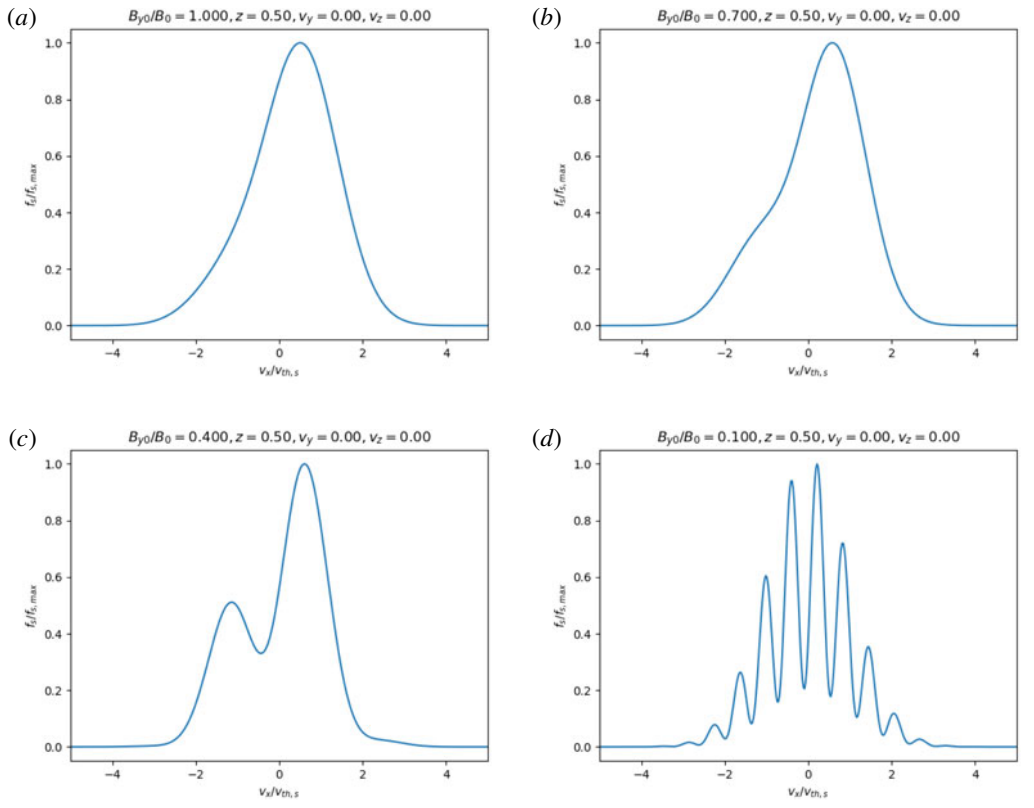

FIGURE 2. Variation of the DF with $v_x/v_{th,s}$ for four different values of B_{y0}/B_0: panel (*a*) $B_{y0}/B_0 = 1.0$, panel (*b*) $B_{y0}/B_0 = 0.7$, panel (*c*) $B_{y0}/B_0 = 0.4$, panel (*d*) $B_{y0}/B_0 = 0.1$. Here, each DF has been normalised by its maximum value and we have chosen $z/L = 0.5$ and $v_y = v_z = 0$.

condition to vanish identically (this is a pre-requisite for being able to apply the method by Channell (1976)). Hence, in the limit $B_{y0} \to 0$ a_s does not go to zero, but to ∞, which is unacceptable for the distribution function. For finite B_{y0}, a_s is finite but it increases rapidly as a function of B_{y0}.

This leads to further unwanted properties of the DF, which we illustrate in figures 2 and 3. Figure 2 shows the DF as a function of $v_x/v_{th,s}$, for $z/L = 0.5$ and $v_y = v_z = 0$, and how it changes as B_{y0}/B_0 decreases from 1.0 to 0.1. The maximum values of the DFs in figure 2 are normalised to unity (i.e. we have divided the DFs by their maximum value for a given ratio B_{y0}/B_0). As one can clearly see in figure 2 the DF develops more and more maxima and minima in the v_x-direction, due to the dominance of the cosine term in the distribution function caused by the increase in a_s. It must be suspected that this filamentation in velocity space might lead to instabilities. We also point out that the parameter b_s has to increase as well so that $b_s > a_s$ to keep the DF positive (in the plots we have used $b_s = 1.5\, a_s$). Figure 3 shows on a logarithmic scale how the maximum value of the DF (for the fixed values of z, v_y and v_z) increases dramatically as B_{y0}/B_0 decreases.

Taken together his clearly shows not only that the limit $B_{y0}/B_0 \to 0$ does not exist and that hence there is no smooth transition to the Harris sheet DF, but that the family

https://doi.org/10.1017/S0022377820000604 Published online by Cambridge University Press

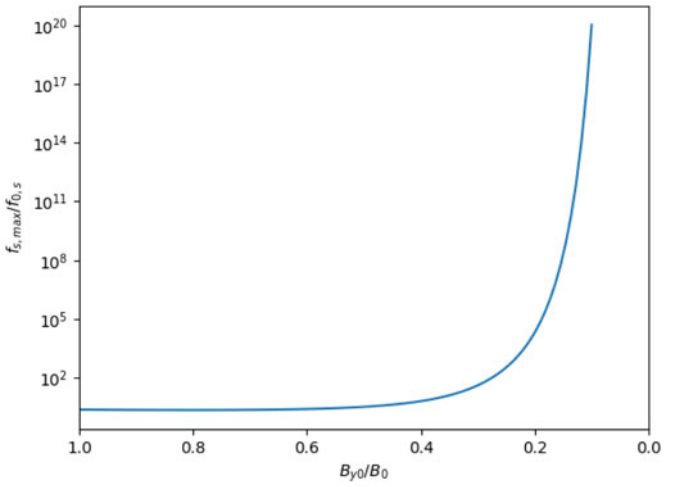

FIGURE 3. Variation of the DF maximum with B_{y0}/B_0.

of DFs will not be very useful even for finite, but small values of the ratio B_{y0}/B_0. The question that arises is: can one find a family of VM equilibrium DFs which provides a smooth transition from the force-free Harris sheet to the Harris sheet?

4. Alternative intermediate cases

In this section, we will consider an alternative magnetic field profile to that in (2.2), of the form

$$\boldsymbol{B}(z) = B_0 \left(\tanh(z/L), \frac{\lambda}{\cosh(\lambda z/L)}, 0 \right), \tag{4.1}$$

where we have defined the abbreviation

$$\lambda = \frac{B_{y0}}{B_0}. \tag{4.2}$$

A similar, albeit not totally identical magnetic field profile has previously been used by Huang *et al.* (2017) to study instabilities using this type of collisionless current sheet. We will show that this magnetic field profile can be used to consistently describe a transition from the Harris sheet to the force-free Harris sheet.

For completeness we here also state the current density and zz-component if the pressure tensor associated with this field, which are given by

$$\boldsymbol{j}(z) = \frac{B_0}{\mu_0 L} \left(\frac{\lambda^2 \sinh(\lambda z/L)}{\cosh^2(\lambda z/L)}, \frac{1}{\cosh^2(z/L)}, 0 \right), \tag{4.3}$$

$$P_{zz}(z) = \frac{B_0^2}{2\mu_0} \left[\frac{1}{\cosh^2(z/L)} + \lambda^2 \left(1 - \frac{1}{\cosh^2(\lambda z/L)} \right) \right] + P_{b2}, \tag{4.4}$$

respectively, where $P_{b2} \geqslant 0$ is a constant background pressure. We remark that we have written the non-background part of the pressure in such a way that it is always positive, regardless of the value of the positive constant P_{b2}.

https://doi.org/10.1017/S0022377820000604 Published online by Cambridge University Press

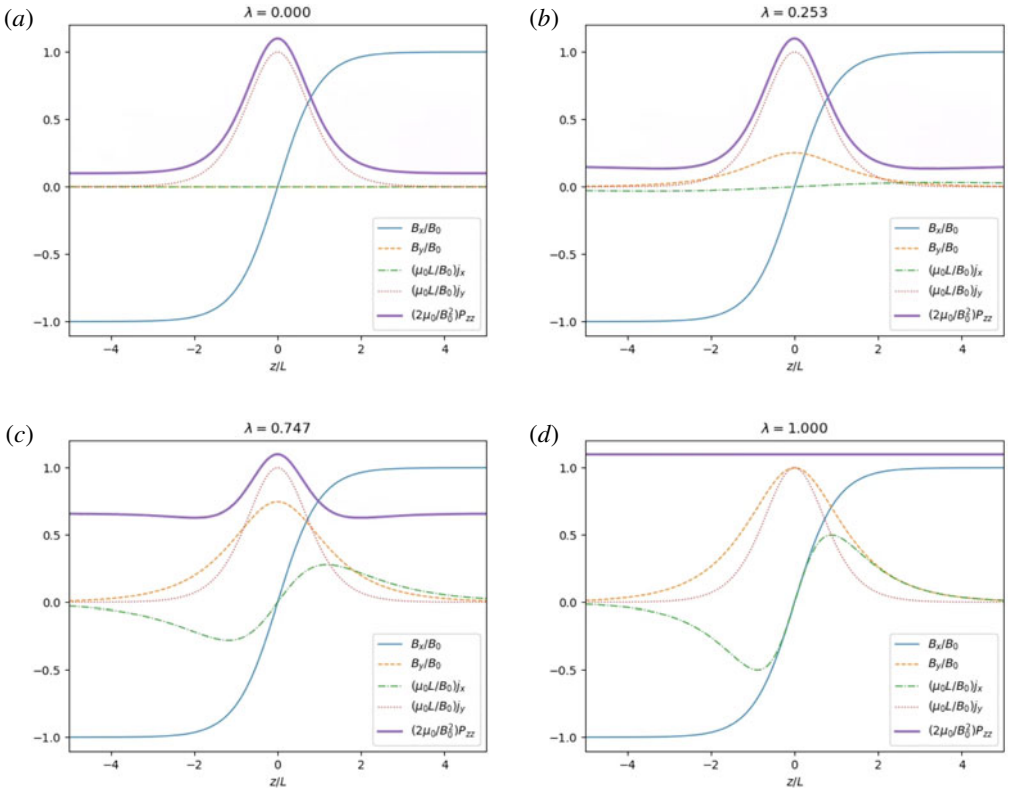

FIGURE 4. Magnetic field, pressure and current density for the alternative intermediate cases with (*a*) $\lambda = 0.0$, (*b*) $\lambda = 0.253$, (*c*) $\lambda = 0.747$ and (*d*) $\lambda = 1.0$. The only noticeable change compared to the profiles shown in figure 1 are the slight dips (minima) in the pressure profile at the edge of the current sheet. The changes in the B_y and j_x profiles are not immediately obvious without direct comparison.

For $\lambda = 0$, the magnetic field (4.1) becomes the Harris sheet field, and for $\lambda = 1$ it becomes the force-free Harris sheet field. Setting $P_b = P_{b2} + B_0^2/2\mu_0$ in (2.3) for $\lambda = 1$ ($B_{y0} = B_0$) will make the two pressure functions equal in that case. The range $0 < \lambda < 1$ can be thought of as describing intermediate fields between the Harris and force-free Harris sheets, although the guide field and pressure profile deviates from the previous intermediate cases. Figure 4 shows magnetic field, pressure and current density profiles for the Harris sheet ($\lambda = 0.0$), two intermediate cases with $\lambda = 0.253$ and $\lambda = 0.747$ and the force-free Harris sheet ($\lambda = 1.0$). The background pressure has been chosen in the same way as for figure 1. The only obvious difference to the plots shown in figure 1 are the slight dips in the pressure profile (local minima) at the edges of the current sheet. On comparison with figure 1, we also see that decreasing λ results in a widening of the B_y profile, due to the λ factor inside the $[\cosh(\lambda z/L)]^{-1}$ in the y-component of (4.1). The amplitude of B_y decreases in the same way as in the other case as λ decreases, and eventually heads to zero as $\lambda \to 0$.

It is straightforward to show that this macroscopic magnetic field profile is consistent with the DF in (3.4). One could suspect that this leads to the same problem with the limit $B_{y0} \to 0$ as before, but when checking the constraints on the

https://doi.org/10.1017/S0022377820000604 Published online by Cambridge University Press

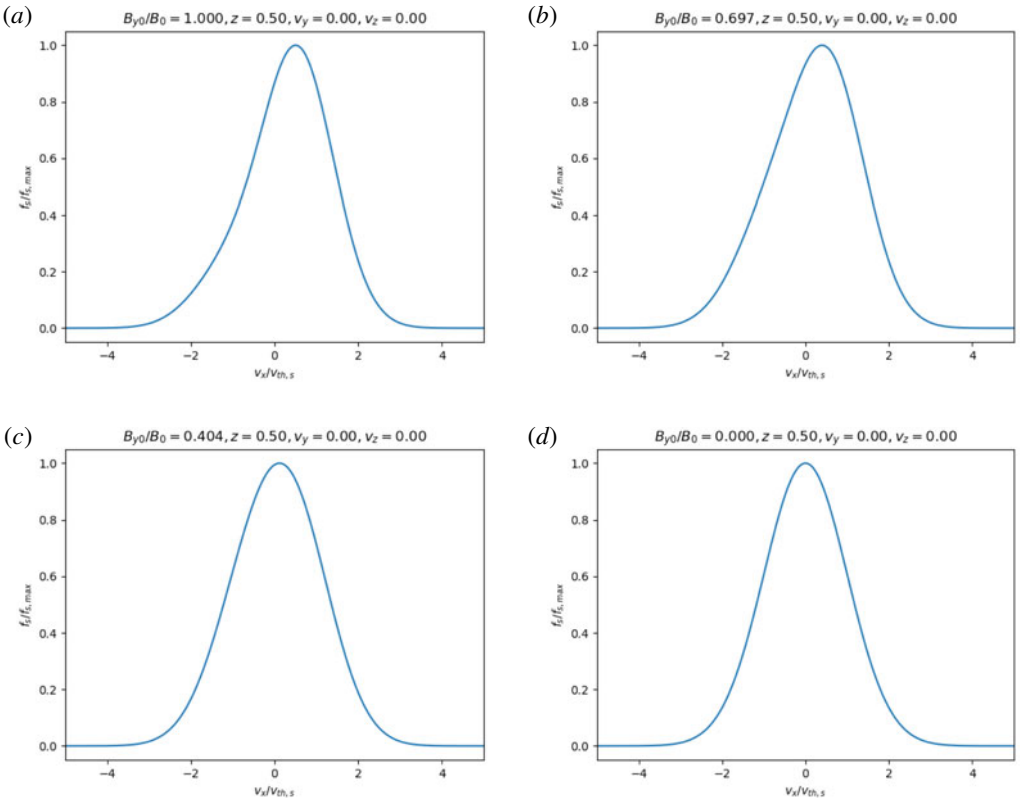

FIGURE 5. Variation of the DF with $v_x/v_{th,s}$ for different values of $\lambda = B_{y0}/B_0$. Here, the DF has been normalised by its maximum value and we have chosen $z/L = 0.5$ and $v_y = v_z = 0$. As one can see there is very little change as λ decreases.

parameters of the DF one finds that while one still has

$$a_s = \lambda^2 \exp\left(\frac{u_{xs}^2}{2v_{th,s}^2}\right) \exp\left(\frac{u_{ys}^2}{2v_{th,s}^2}\right), \tag{4.5}$$

as before, the condition for u_{xs} has changed to

$$u_{xs}^2 = \frac{4\lambda^2}{B_{y0}^2 \beta_s^2 q_s^2 L^2} = \frac{4}{B_0^2 \beta_s^2 q_s^2 L^2}, \tag{4.6}$$

which no longer varies with B_{y0}. Therefore, in this case we indeed find that $\lambda \to 0$ implies $a_s \to 0$, as desired.

It is, however, prudent to also have a look at the DFs and their maximum value as $\lambda \to 0$. We show plots of the variation of the DF with v_x (for $z/L = 0.5$ and $v_y = v_z = 0$) in figure 5, for decreasing values of λ. For this case we can actually take the limit $\lambda \to 0$ without any problem (see panel *d*). As in figure 2, we have normalised each DF to its maximum value. The variation of this maximum value with decreasing λ is shown in figure 6. For this case the maximum of the DF actually decreases as λ and hence B_{y0} decreases. With a relatively simple modification of the magnetic field profile we have managed to eliminate the singular limit.

https://doi.org/10.1017/S0022377820000604 Published online by Cambridge University Press

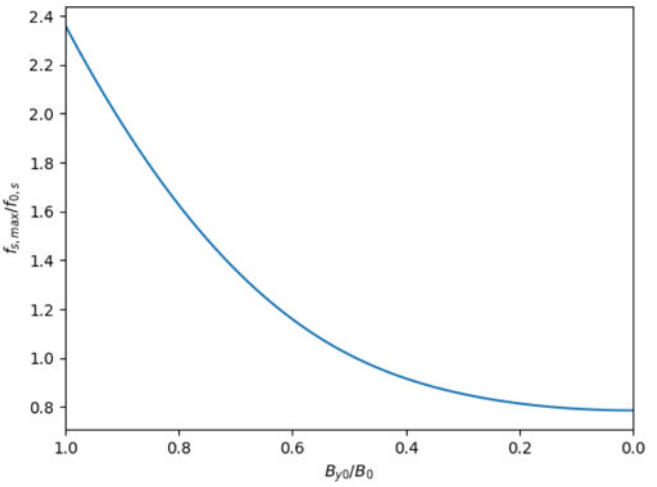

FIGURE 6. Variation of the maximum of the DF with B_{y0}/B_0 for the alternative magnetic field profile. As one can see the maximum decreases with decreasing λ and it does not diverge in the limit $\lambda \to 0$. In contrast to figure 3 here a linear scale can be used for the plot.

5. Summary and conclusions

In this paper, we have discussed collisionless current sheet equilibria that are intermediate cases between the Harris sheet (current density perpendicular to magnetic field direction) and the force-free Harris sheet (current density exactly parallel to the magnetic field direction). Such a family of Vlasov–Maxwell equilibrium DF had already been briefly mentioned in Harrison & Neukirch (2009*a*). However, as the more detailed investigation presented in this paper shows, this family of DFs is of limited usefulness due to the fact that first of all the limit of the guide field amplitude $B_{y0} \to 0$ is singular in the sense that the maximum of the DF tends to ∞ and that with decreasing B_{y0} the velocity space structure of the DF in the v_x direction becomes more and more filamentary. We proposed an alternative family of intermediate collisionless current sheet equilibria with a magnetic guide field that has a slightly modified spatial structure. Formally, the DFs associated with this magnetic field remain the same, but the constraints imposed on the DF parameters by the self-consistency condition now allow the maximum value of the DFs to remain not only finite, but at a reasonable level as $B_{y0} \to 0$.

We consider it important both from a theoretical and from a modelling and observational point of view that reasonable self-consistent equilibria of collisionless current sheets are available not only for the two limiting cases of force-free Harris sheet and normal Harris sheet. While some observations can be explained by, for example, force-free current sheet models (e.g. Panov *et al.* 2011; Artemyev, Angelopoulos & Vasko 2019*a*; Artemyev *et al.* 2019*b*; Neukirch *et al.* 2020), it is to be expected that versions of the intermediate current sheet models are encountered with a greater likelihood than the limiting cases.

Acknowledgements

The authors acknowledge the support of the Science and Technology Facilities Council (STFC) via the consolidated grants ST/K000950/1, ST/N000609/1 and

ST/S000402/1 (T.N. and F.W.) and the Natural Environment Research Council (NERC) Highlight Topic grant no. NE/P017274/1 (Rad-Sat) (O.A.). T.N. and F.W. would also like to thank the University of St Andrews for general financial support.

Editor Francesco Califano thanks the referees for their advice in evaluating this article.

REFERENCES

ABRAHAM-SHRAUNER, B. 2013 Force-free Jacobian equilibria for Vlasov–Maxwell plasmas. *Phys. Plasmas* **20**, 102117.

ALLANSON, O., NEUKIRCH, T., TROSCHEIT, S. & WILSON, F. 2016 From one-dimensional fields to Vlasov equilibria: theory and application of Hermite polynomials. *J. Plasma Phys.* **82**, 905820306.

ALLANSON, O., NEUKIRCH, T., WILSON, F. & TROSCHEIT, S. 2015 An exact collisionless equilibrium for the force-free Harris sheet with low plasma beta. *Phys. Plasmas* **22**, 102116.

ALPERS, W. 1969 Steady state charge neutral models of the magnetopause. *Astrophys. Space Sci.* **5**, 425–437.

ARTEMYEV, A. V., ANGELOPOULOS, V. & VASKO, I. Y. 2019*a* Kinetic properties of solar wind discontinuities at 1 AU observed by ARTEMIS. *J. Geophys. Res.* **124**, 3858–3870.

ARTEMYEV, A. V., ANGELOPOULOS, V., VASKO, I. Y., RUNOV, A., AVANOV, L. A., GILES, B. L., RUSSELL, C. T. & STRANGEWAY, R. J. 2019*b* On the kinetic nature of solar wind discontinuities. *Geophys. Res. Lett.* **46**, 1185–1194.

ATTICO, N. & PEGORARO, F. 1999 Periodic equilibria of the Vlasov–Maxwell system. *Phys. Plasmas* **6**, 767–770.

BOBROVA, N. A., BULANOV, S. V., SAKAI, J. I. & SUGIYAMA, D. 2001 Force-free equilibria and reconnection of the magnetic field lines in collisionless plasma configurations. *Phys. Plasmas* **8**, 759–768.

BOWERS, K. & LI, H. 2007 Spectral energy transfer and dissipation of magnetic energy from fluid to kinetic scales. *Phys. Rev. Lett.* **98**, 035002.

CHANNELL, P. J. 1976 Exact Vlasov–Maxwell equilibria with sheared magnetic fields. *Phys. Fluids* **19**, 1541–1545.

CORREA-RESTREPO, D. & PFIRSCH, D. 1993 Negative-energy waves in an inhomogeneous force-free Vlasov plasma with sheared magnetic field. *Phys. Rev.* E **47**, 545–563.

DAUGHTON, W. & KARIMABADI, H. 2007 Collisionless magnetic reconnection in large-scale electron–positron plasmas. *Phys. Plasmas* **14**, 072303.

DAUGHTON, W., ROYTERSHTEYN, V., KARIMABADI, H., YIN, L., ALBRIGHT, B. J., BERGEN, B. & BOWERS, K. J. 2011 Role of electron physics in the development of turbulent magnetic reconnection in collisionless plasmas. *Nat. Phys.* **7**, 539–542.

DORVILLE, N., BELMONT, G., AUNAI, N., DARGENT, J. & REZEAU, L. 2015 Asymmetric kinetic equilibria: generalization of the BAS model for rotating magnetic profile and non-zero electric field. *Phys. Plasmas* **22**, 092904.

FAN, F., HUANG, C., LU, Q., XIE, J. & WANG, S. 2016 The structures of magnetic islands formed during collisionless magnetic reconnections in a force-free current sheet. *Phys. Plasmas* **23**, 112106.

GUO, F., LI, H., DAUGHTON, W., LI, X. & LIU, Y.-H. 2016*a* Particle acceleration during magnetic reconnection in a low-beta pair plasma. *Phys. Plasmas* **23**, 055708.

GUO, F., LI, H., DAUGHTON, W. & LIU, Y.-H. 2014 Formation of hard power laws in the energetic particle spectra resulting from relativistic magnetic reconnection. *Phys. Rev. Lett.* **113**, 155005.

GUO, F., LI, X., LI, H., DAUGHTON, W., ZHANG, B., LLOYD-RONNING, N., LIU, Y.-H., ZHANG, H. & DENG, W. 2016*b* Efficient Production of high-energy nonthermal particles during magnetic reconnection in a magnetically dominated ion–electron plasma. *Astrophys. J. Lett.* **818**, L9.

GUO, F., LIU, Y.-H., DAUGHTON, W. & LI, H. 2015 Particle acceleration and plasma dynamics during magnetic reconnection in the magnetically dominated regime. *Astrophys. J.* **806**, 167.

HARRIS, E. G. 1962 On a plasma sheath separating regions of oppositely directed magnetic field. *Nuovo Cimento* **23**, 115.

HARRISON, M. G. & NEUKIRCH, T. 2009*a* One-dimensional Vlasov–Maxwell equilibrium for the force-free Harris sheet. *Phys. Rev. Lett.* **102**, 135003.

HARRISON, M. G. & NEUKIRCH, T. 2009*b* Some remarks on one-dimensional force-free Vlasov–Maxwell equilibria. *Phys. Plasmas* **16**, 022106.

HESSE, M. 2006 Dissipation in magnetic reconnection with a guide magnetic field. *Phys. Plasmas* **13**, 122107.

HESSE, M., BIRN, J. & KUZNETSOVA, M. 2001 Collisionless magnetic reconnection: electron processes and transport modeling. *J. Geophys. Res.* **106**, 3721–3736.

HESSE, M., KUZNETSOVA, M. & BIRN, J. 2004 The role of electron heat flux in guide-field magnetic reconnection. *Phys. Plasmas* **11**, 5387–5397.

HESSE, M., KUZNETSOVA, M., SCHINDLER, K. & BIRN, J. 2005 Three-dimensional modeling of electron quasiviscous dissipation in guide-field magnetic reconnection. *Phys. Plasmas* **12**, 100704.

HESSE, M., NEUKIRCH, T., SCHINDLER, K., KUZNETSOVA, M. & ZENITANI, S. 2011 The diffusion region in collisionless magnetic reconnection. *Space Sci. Rev.* **160**, 3–23.

HESSE, M., SCHINDLER, K., BIRN, J. & KUZNETSOVA, M. 1999 The diffusion region in collisionless magnetic reconnection. *Phys. Plasmas* **6**, 1781–1795.

HUANG, F., XU, J., YAN, F., ZHANG, M. & YU, M. Y. 2017 Instabilities of current-sheet with a nonuniform guide field. *Phys. Plasmas* **24**, 092104.

KOCHAROVSKY, V. V., KOCHAROVSKY, V. V., MARTYANOV, V. Y. & TARASOV, S. V. 2016 Analytical theory of self-consistent current structures in a collisionless plasma. *Phys. Uspekhi* **59**, 1165–1210.

KOLOTKOV, D. Y., VASKO, I. Y. & NAKARIAKOV, V. M. 2015 Kinetic model of force-free current sheets with non-uniform temperature. *Phys. Plasmas* **22**, 112902.

KUZNETSOVA, M. M., HESSE, M. & WINSKE, D. 1998 Kinetic quasi-viscous and bulk flow inertia effects in collisionless magnetotail reconnection. *J. Geophys. Res.* **103**, 199–214.

KUZNETSOVA, M. M., HESSE, M. & WINSKE, D. 2000 Toward a transport model of collisionless magnetic reconnection. *J. Geophys. Res.* **105**, 7601–7616.

KUZNETSOVA, M. M., HESSE, M. & WINSKE, D. 2001 Collisionless reconnection supported by nongyrotropic pressure effects in hybrid and particle simulations. *J. Geophys. Res.* **106**, 3799–3810.

LIU, Y.-H., DAUGHTON, W., KARIMABADI, H., LI, H. & ROYTERSHTEYN, V. 2013 Bifurcated structure of the electron diffusion region in three-dimensional magnetic reconnection. *Phys. Rev. Lett.* **110**, 265004.

MORATZ, E. & RICHTER, E. W. 1966 Elektronen-Geschwindigkeitsverteilungsfunktionen für kraftfreie bzw. teilweise kraftfreie Magnetfelder. *Z. Naturforsch.* A **21**, 1963.

MOTTEZ, F. 2003 Exact nonlinear analytic Vlasov–Maxwell tangential equilibria with arbitrary density and temperature profiles. *Phys. Plasmas* **10**, 2501–2508.

MYNICK, H. E., SHARP, W. M. & KAUFMAN, A. N. 1979 Realistic Vlasov slab equilibria with magnetic shear. *Phys. Fluids* **22**, 1478–1484.

NEUKIRCH, T., VASKO, I. Y., ARTEMYEV, A. V. & ALLANSON, O. 2020 Kinetic models of tangential discontinuities in the solar wind. *Astrophys. J.* **891**, 86.

NEUKIRCH, T., WILSON, F. & ALLANSON, O. 2018 Collisionless current sheet equilibria. *Plasma Phys. Control. Fusion* **60**, 014008.

NEUKIRCH, T., WILSON, F. & HARRISON, M. G. 2009 A detailed investigation of the properties of a Vlasov–Maxwell equilibrium for the force-free Harris sheet. *Phys. Plasmas* **16**, 122102.

NISHIMURA, K., GARY, S. P., LI, H. & COLGATE, S. A. 2003 Magnetic reconnection in a force-free plasma: simulations of micro- and macroinstabilities. *Phys. Plasmas* **10**, 347–356.

PANOV, E. V., ARTEMYEV, A. V., NAKAMURA, R. & BAUMJOHANN, W. 2011 Two types of tangential magnetopause current sheets: cluster observations and theory. *J. Geophys. Res.* **116**, A12204.

PRITCHETT, P. L. 2001 Geospace environment modeling magnetic reconnection challenge: simulations with a full particle electromagnetic code. *J. Geophys. Res.* **106**, 3783–3798.

PRITCHETT, P. L. 2005 Onset and saturation of guide-field magnetic reconnection. *Phys. Plasmas* **12** (6), 062301.

PRITCHETT, P. L. & CORONITI, F. V. 2004 Three-dimensional collisionless magnetic reconnection in the presence of a guide field. *J. Geophys. Res.* **109**, 1220.

RICCI, P., BRACKBILL, J. U., DAUGHTON, W. & LAPENTA, G. 2004 Collisionless magnetic reconnection in the presence of a guide field. *Phys. Plasmas* **11**, 4102–4114.

ROGERS, B. N., DENTON, R. E. & DRAKE, J. F. 2003 Signatures of collisionless magnetic reconnection. *J. Geophys. Res.* **108**, 1111.

ROTH, M., DE KEYSER, J. & KUZNETSOVA, M. M. 1996 Vlasov theory of the equilibrium structure of tangential discontinuities in space plasmas. *Space Sci. Rev.* **76**, 251–317.

SCHINDLER, K. 2007 *Physics of Space Plasma Activity*. Cambridge University Press.

SESTERO, A. 1967 Self-consistent description of a warm stationary plasma in a uniformly sheared magnetic field. *Phys. Fluids* **10**, 193–197.

SHAY, M. A., DRAKE, J. F., DENTON, R. E. & BISKAMP, D. 1998 Structure of the dissipation region during collisionless magnetic reconnection. *J. Geophys. Res.* **103**, 9165–9176.

VASKO, I. Y., ARTEMYEV, A. V., PETRUKOVICH, A. A. & MALOVA, H. V. 2014 Thin current sheets with strong bell-shape guide field: cluster observations and models with beams. *Ann. Geophys.* **32**, 1349–1360.

WAN, W., LAPENTA, G., DELZANNO, G. L. & EGEDAL, J. 2008 Electron acceleration during guide field magnetic reconnection. *Phys. Plasmas* **15**, 032903.

WILSON, F. & NEUKIRCH, T. 2011 A family of one-dimensional Vlasov–Maxwell equilibria for the force-free Harris sheet. *Phys. Plasmas* **18**, 082108.

WILSON, F., NEUKIRCH, T. & ALLANSON, O. 2017 Force-free collisionless current sheet models with non-uniform temperature and density profiles. *Phys. Plasmas* **24**, 092105.

WILSON, F., NEUKIRCH, T. & ALLANSON, O. 2018 Collisionless distribution functions for force-free current sheets: using a pressure transformation to lower the plasma beta. *J. Plasma Phys.* **84**, 905840309.

WILSON, F., NEUKIRCH, T., HESSE, M., HARRISON, M. G. & STARK, C. R. 2016 Particle-in-cell simulations of collisionless magnetic reconnection with a non-uniform guide field. *Phys. Plasmas* **23**, 032302.

ZELENYI, L. M., MALOVA, H. V., ARTEMYEV, A. V., POPOV, V. Y. & PETRUKOVICH, A. A. 2011 Thin current sheets in collisionless plasma: equilibrium structure, plasma instabilities, and particle acceleration. *Plasma Phys. Rep.* **37**, 118–160.

ZHOU, F., HUANG, C., LU, Q., XIE, J. & WANG, S. 2015 The evolution of the ion diffusion region during collisionless magnetic reconnection in a force-free current sheet. *Phys. Plasmas* **22**, 092110.